

# Dissociation between *in vitro* and *in vivo* epileptogenicity in a rat model of cortical dysplasia

Christoph Kellinghaus<sup>1,3</sup>, Gabriel Möddel<sup>1,3</sup>, Hiroshi Shigeto<sup>1</sup>, Zhong Ying<sup>1</sup>, Berit Jacobsson<sup>1</sup>, Jorge Gonzalez-Martinez<sup>2</sup>, Candice Burrier<sup>1</sup>, Damir Janigro<sup>2</sup>, Imad M. Najm<sup>1</sup>

<sup>1</sup> Department of Neurology,

<sup>2</sup> Department of Neurological Surgery, The Cleveland Clinic Foundation, Cleveland, Ohio, USA

<sup>3</sup> Dept. of Neurology, University of Münster, Münster, Germany

Authors Christoph Kellinghaus and Gabriel Möddel contributed equally to this study

Received August 17, 2006; Accepted October 16, 2006

**ABSTRACT – Objective.** Malformations of cortical development are frequent causes of human refractory epilepsy. The freeze-lesion model in rats shows histopathological features similar to those found in human polymicrogyria. Previous studies reported *in vitro* hyperexcitability in this model, but *in vivo* epileptogenicity has not been confirmed.

**Methods.** Neocortical freeze lesions were induced in Sprague-Dawley rat pups (n = 10) on postnatal day 0 or 1 (P0/P1). Sham-operated animals served as controls (n = 10). On P60, animals were implanted with epidural electrodes for long-term video-EEG monitoring (4 weeks). The threshold for pentylentetrazol-induced seizures was determined. Animals were sacrificed and brain sections processed for histological staining and *in vitro* electrophysiological recordings. Epileptiform field potential repetition rate, amplitude and integral were compared between slices containing a cortical freeze lesion, and slices from sham-operated rats.

**Results.** No interictal spikes and no electrographic or clinical seizures occurred in either group. The median threshold for pentylentetrazol-induced seizures was 60 mg/kg for lesioned, and 45 mg/kg for control animals (difference not significant). No spontaneous epileptiform field potentials were recorded from either freeze-lesion or control slices bathed in normal, artificial cerebrospinal fluid (ACSF). Upon omission of Mg<sup>2+</sup> from the bath, epileptiform field potentials were elicited that showed a significantly higher burst integral in the freeze lesion slices compared to control slices.

**Conclusion.** Neocortical freeze lesions induced in newborn rat pups show histological characteristics reminiscent of human cortical dysplasia. Brain slices containing neocortical freeze lesions display hyperexcitability *in vitro*, but the same lesion does not appear to show spontaneous epileptogenicity *in vivo*.

**Key words:** cortical dysplasia, freeze lesion, electroencephalography, epileptogenicity

**Correspondence:**

Christoph Kellinghaus, MD  
Dept. of Neurology  
University Hospitals Münster  
Albert-Schweitzer-Straße 33  
48149 Münster  
Germany  
Tel: (+00 49) 251 83 48196  
Fax: (+00 49) 251 83 48181  
<kelling@uni-muenster.de>

doi: 10.1684/epd.2007.0061

Malformations of cortical development (MCD) are among the most common pathological causes of medically refractory focal epilepsy in patients undergoing surgical resection (Annegers, 1994, Tassi *et al.* 2002). Post-surgical seizure-free outcome is less favorable in patients with MCD than in patients with other lesions, e.g. hippocampal sclerosis (Bast *et al.* 2006, Hamiwka *et al.* 2005, Lüders and Schuele, 2006, Wyllie *et al.* 1998).

However, reliable data about the pathophysiological mechanisms resulting in epilepsy in these patients remain scarce. Several animal models of MCD have been investigated, such as the focal freeze lesion model (Dvorak and Feit, 1977, Rosen *et al.* 1992), the *in utero* alkylating (MAM) model (Baraban and Schwartzkroin, 1995), and the *in utero* irradiation model (Roper *et al.* 1995), as well as genetic models (Amano *et al.* 1996 ; Chae *et al.* 1997). Among the injury-inducing models, spontaneous but rare seizures have only been demonstrated in the *in utero* irradiation and alkylating models (Kellinghaus *et al.* 2004, Kondo *et al.* 2001, Möddel *et al.* unpublished observations).

In addition, the anatomical changes in these 2 *in utero* models are multifocal (affecting both the archi-hippocampal formations and neocortex) and only remotely resemble the characteristics of focal cortical dysplasia in humans (Prayson and Estes, 1995, Taylor *et al.* 1971).

In contrast, neocortical lesions induced by application of a freeze metal probe on neonatal rat pup skull ("freeze lesions") share several anatomical and histological features with focal polymicrogyria in humans (Dvorak *et al.* 1978, Rosen *et al.* 1992). Freeze-lesioned neocortical brain slices have been extensively studied *in vitro* and were found to display hyperexcitability (Chevassus-Au-Louis *et al.* 1999, Jacobs *et al.* 1999a, Redecker *et al.* 2005). However, long-term, video electroencephalographic (EEG) recordings have not yet been performed using this model. Holmes (Holmes *et al.* 1999) found no difference in afterdischarge threshold and kindling rate in young freeze-lesioned rats as compared to controls. Thus, the clinical relevance of the anatomic and *in vitro* findings remains unclear.

This study was designed to investigate whether rats with neocortical freeze lesions display *in vivo* epileptogenicity, and to study the threshold of their response to a seizure-provoking agent (as compared to control animals). Furthermore, we aimed to correlate the *in vivo* observations with histological and *in vitro* electrophysiological findings.

## Methods

### Animals

Neocortical freeze lesions were induced in rats as initially described by Dvorak and Feit (Dvorak and Feit, 1977) with slight modifications. Newborn (post-natal day 0 or 1;

PN0/1) Sprague-Dawley rat pups (n = 16; parent animals from Charles River, Wilmington, MA, USA) were anesthetized by hypothermia (5 minutes on dry ice covered by a plastic cover). A 6-7 mm incision was made in the skin overlying the fronto-parietal cortex. After exposing the skull, a cold probe was placed on the skull covering the left primary motor and somatosensory cortex on three separate points along a line approximately 1 mm lateral from the midline for 8 seconds per contact. The cold probe consisted of a stainless steel rod of approximately 100 mm length and a contact surface of approximately 2 x 1 mm. It was cooled to -60°C in a methanol-filled centrifuge tube placed in dry ice. Following this procedure, the skin was closed with a single suture, and the animals were placed under a heat lamp and returned to their mother after 30 minutes. The control animals (n = 12) were treated in the same way with the exception that the steel probe was at room temperature (21-23°C). Rat pups remained with their mothers until they were weaned at PN21. All animals were maintained on a 12-hour light-dark cycle with food and water available *ad libitum* throughout the whole time, including the EEG recordings. The research protocol was approved by the Cleveland Clinic Foundation institutional animal care and use committee (IACUC).

### Electrode implantation

After PN60, stereotactic electrode implantations were performed in 10 freeze-lesioned rats (8 males, 2 females) and 10 control rats (8 males, 2 females) under pentobarbital anesthesia (50 mg/kg, intraperitoneal, *i.p.*), using the Kopf stereotactic frame according to coordinates that were adapted from Paxinos' stereotactic atlas of the rat brain (Paxinos, 1986). After preparation of the skull, stainless steel screw electrodes (MX-0090-2, Small Parts Inc., Miami, Florida) were placed bilaterally on the dura mater of the frontal cortex (LF: left frontal cortex, RF: right frontal cortex, A: 1.0 mm, L: ± 2.5 mm from the bregma) and the parietal cortex (LP: left parietal cortex, RP: right parietal cortex, P: 2.0 mm, L: ± 2.5 mm from the bregma). An additional screw electrode was placed in the frontal sinus and served as a reference recording electrode. The electrodes were connected to a plastic plug (SMP-06V-BC, Japan Solderless Terminal MFG., Tokyo, Japan) which was fixed to the skull using dental cement (Hygenic repair resin, Hygenic, Akron, OH, USA). In order to maintain electrodes and plugs in position for long-time monitoring, an extracranial fixation technique was employed (Mascott *et al.* 1994): a stainless steel suture (0.1 mm diameter) was wrapped around the posterior limb of the zygomatic arches after careful preparation of the temporalis muscles off the lateral skull surfaces. The steel suture was then embedded in the dental cement to anchor the electrodes and plug into the zygomatic arches. Rats were left unrestrained for 1 week for recovery from surgery before prolonged EEG recordings were performed.

### Prolonged EEG monitoring

Continuous digital EEG recordings from freeze-lesioned rats and the sham-operated control animals were performed in five custom-made, electrically shielded boxes with free access to food and water. Implanted recording electrodes were connected to pendulous electroslip rings (MRS 35-06P, M-T GIKEN, Tokyo, Japan). This arrangement allowed the acquisition of real-time low-noise EEGs of the freely moving animals 24 hours per day. Monitoring of the rats was performed in 24-hour periods of recordings alternating with 24-hour periods without EEG recordings. The freeze-lesioned animals underwent a total of 28 days of monitoring (14 days before and 14 days after seizure threshold determination), the control animals were monitored for a total of 15 days (1 day before and 14 days after seizure threshold determination).

Five-channel digital EEG recordings were performed using the Vanguard system (Lamont, Madison, WI, USA), consisting of a recording Hewlett-Packard workstation and a similar review system. A total of five rats were monitored simultaneously at any given time. EEG filter settings were: 1 Hz (low frequency filter) and 70 Hz (high frequency filter), sampling frequency was 100 Hz. Each cage was monitored with a digital video-camera fixed just in front of the cage. The time relationships between EEG events and clinical motor fits were assessed using a split-screen video monitoring system. The simultaneously-obtained EEG and video data were digitally stored in the hard drive of the recording workstation and later transferred to magneto-optical disks (MO).

### Data analyses

The digitized EEG signals were reformatted to referential and bipolar montages. The EEG was analyzed by visual inspection for the presence of interictal and ictal epileptic activities. Interictal spikes were defined as sharp potential fluctuations with durations of between 20 and 150 ms and amplitudes of at least 5 times the background EEG activity. The interictal spikes were mapped to the area of maximum amplitude (on referential montages) and to the electrode of phase reversal (on bipolar montages) according to their location. The rates of occurrence of all interictal spikes were calculated and expressed as spikes/hour.

As previously described, EEG seizures were defined as rhythmic spiking or paroxysmal fast activity (15-25 Hz) that evolved in amplitude and/or frequency and lasted for at least 10 seconds. The rates of occurrence of ictal activity were calculated and expressed as seizure/day.

Behavioral seizures during the determination of the threshold for PTZ-induced seizures were graded according to the clinical manifestations on a scale modified from Racine (Racine, 1972): Grade 1: facial twitching, Grade 2: facial and forelimb twitching, Grade 3: axial twitching, Grade 4: generalized tonic-clonic seizure with preserva-

tion of posture, Grade 5: generalized tonic-clonic seizure with loss of postural balance.

Statistical testing was performed with a commercially available software package (SPSS 11.0 for Windows, SPSS Inc., Chicago, Illinois, USA). We used the Wilcoxon rank-sum test for inter-group comparison of interval- or ordinal-scaled data. Categorical variables were compared with the Chi-square test or Fisher's exact test (2 x 2 tables). Significance levels were set at  $p = 0.05$  (two-tailed tests).

### Determination of the threshold for PTZ-induced seizures

The implanted animals ( $n = 10$  per group) received a subthreshold PTZ dose of 10 mg/kg *i.p.* If there was no seizure of at least Grade 4 after 10 minutes, additional injections in 5 mg/kg PTZ increments were given once every 10 minutes until a seizure of at least Grade 4 occurred. The total dose needed to elicit a seizure of at least Grade 4 was defined as the threshold PTZ dose.

### Histopathological examination

At the end of the EEG acquisition periods, rats were deeply anesthetized with pentobarbital (60 mg/kg, *i.p.*) and perfused intracardially with 4% paraformaldehyde (PFA) in phosphate-buffered solution (PBS, pH 7.4). The brains were saved in 4% PFA for 2 days and then transferred to 20% sucrose for 48 hours before processing. Serial sections (50  $\mu\text{m}$ ) were cut in the coronal plane using a cryostat. One out of 10 sections was cresylecht violet (CV) Nissl stained for histological examinations. Sections from the animals from both groups were analyzed regarding the presence or absence of a typical pathological lesions, and other histological abnormalities.

### Slice electrophysiology

Freeze-lesioned ( $n = 5$ ) and control ( $n = 5$ ) rats (age 110-130 days) were deeply anesthetized with isoflurane, perfused with ice-cold preincubation artificial cerebrospinal fluid (pACSF; containing [in mM]: NaCl 124; KCl 3;  $\text{CaCl}_2$  1;  $\text{MgCl}_2$  1.4;  $\text{NaHCO}_3$  26;  $\text{KH}_2\text{PO}_4$  1.25; glucose 10), and then decapitated. The brains were quickly removed from the skull and immediately placed into ice-cold, oxygenated pACSF. The brainstem and cerebellum as well as the frontopolar regions were dissected. The central section of the cerebral hemisphere containing the macroscopically visible, freeze-lesion-induced microsulcus (or, in controls, the central section of the left hemisphere), including the sensorimotor cortical regions, was subsequently cut in the coronal plain, into slices of 400-500  $\mu\text{m}$  thickness using a vibratome. Slices were kept in a preincubation chamber containing oxygenated (95%  $\text{O}_2$ ; 5%  $\text{CO}_2$ ) pACSF at room temperature and pH 7.4 for one hour. After 60 min of preincubation, the  $\text{Ca}^{2+}$  concentration was increased to 2 mM to reach ion concentrations comparable to *in vivo* conditions (artificial cerebrospinal fluid,

ACSF). For electrophysiological recordings, a slice containing the microsulcus or a control slice was placed in a submerged recording chamber and was constantly superfused with oxygenated ACSF at a flow rate of 3–4 mL/min at room temperature. Extracellular field potentials (FP) were recorded using borosilicate glass micropipettes (0.5–2 M $\Omega$  electrical resistance) filled with ACSF. In slices from freeze-lesioned animals (FL slices), FP were recorded from two sites simultaneously: (1) directly adjacent to the microsulcus, and (2) 8 mm lateral to the microsulcus in the macroscopically normal neocortex.

Signals were acquired in direct current (DC) mode using an Axopatch 200A amplifier (Axon Instruments, Union City, CA, USA) and recorded on a PC using pCLAMP 8.0 software (Axon Instruments, Union City, CA, USA). In order to elicit epileptiform field potentials (EFP), magnesium was omitted from the bath solution (0 Mg<sup>2+</sup> ACSF, “zero-magnesium model”), (Avoli *et al.* 1987, Avoli *et al.* 1991, Mody *et al.* 1987). Slices were placed in 0 Mg<sup>2+</sup> ACSF for at least one hour and until a stable frequency of EFP activity was seen, before any measurements of burst parameters were performed to ensure stable conditions. In order to characterize epileptiform bursting activity, the following measurements were taken: EFP repetition rate (min<sup>-1</sup>), maximum burst amplitude ( $\mu$ V), and the integral of individual EFP bursts (burst integral,  $\mu$ Vs). Data were tested for significance using Wilcoxon’s non-parametric test for unpaired samples.

## Results

### Histopathological abnormalities

The application of a freeze probe to the skull on PN0/1 produced similar, typical focal structural cortical abnormalities in all animals ( $n = 16$ ) including those that were used for EEG recordings. The abnormalities consisted of a longitudinal microgyrus located in parallel to the midline with a length of 2–5 mm, which was clearly visible macroscopically (*figure 1A*) and appeared as a fissure spanning about two thirds of the cortical thickness on low-magnification microscopic images acquired from brain slices during field potential recordings (*figure 1B*) as well as from cresylecht violet-stained histological sections (*figure 1C*). The microscopic architecture was somewhat variable. Two-, three- or four-layered cortices, with a varying degree of loss of normal cortical architecture, were seen. In the most severe form, layers IV–VI were completely destroyed and substituted by scarring. No histopathological abnormalities were seen in the sham-operated rats ( $n = 12$ ) (*figure 1D*).

### Long-term video-EEG monitoring

All freeze-lesioned rats were monitored for 14 days before the determination of the seizure threshold to look for

spontaneous seizures or epileptiform discharges. In addition, all control rats were monitored for 24 hours before the PTZ injection. No seizures or spikes were recorded in any animal of either of the groups during the evaluation period prior to the PTZ injection. One of the rats suffered an injury during the PTZ-induced seizure and was sacrificed immediately afterwards. The other nine freeze-lesioned rats as well as the ten control animals were monitored for 14 days after the threshold determination, beginning immediately after the clinical seizures had occurred. During the first twelve hours following the PTZ-induced seizures, generalized spikes were seen in all animals of both groups. We did not see any differences regarding frequency, localization or morphology between the animals of both groups. The frequency of the spikes decreased over a time-period of 10–12 hours, until no further epileptiform discharges were observed 12 hours after the PTZ injections. We considered these discharges to be an acute PTZ effect and excluded the first 12 hours after PTZ injection from further analyses. Thereafter, no spikes and no seizures were observed in any of the animals in both groups (*figure 2*). The recordings of the two groups showed normal alpha-background activity as well as normal sleep-wake cycles. There was no focal slowing and no evidence for other EEG abnormalities in either group.

### Threshold for PTZ-induced seizures

PTZ was injected step-wise until the animals developed a generalized tonic-clonic seizure (stage IV or V). Seizure stages I or II were reached after injection of a median dose of 37.5 mg/kg body weight in the freeze-lesioned rats, and 40 mg/kg in the control animals. A generalized tonic-clonic seizure (stage IV or V) was elicited after injection of a median dose of 60 mg/kg in the lesioned group, and 45 mg/kg in the control group. The differences were not statistically significant. There were also no significant differences in age or body weight between both groups at the time of the PTZ injection (*table 1*). Practical and technical issues precluded EEG-recording during the threshold-determination for PTZ-induced seizures.

### In vitro electrophysiology

No spontaneous epileptiform field potentials (EFP) were recorded in either hemispheric brain slices containing a cortical freeze lesion (FL slices; 5 animals, one slice per animal) or in brain slices from sham-operated rats (CTRL slices; 5 animals, one slice per animal). Omission of Mg<sup>2+</sup> ions from the bath reliably elicited EFP in both FL and CTRL slices. In FL slices, EFP were simultaneously recorded from the cortex directly adjacent to the freeze-lesion-induced microsulcus (LES, see *figure 2B*), as well as from the cortex 8 mm lateral to the microsulcus (LAT). EFP occurred synchronously at both recording sites, although the temporal relationship between the initial negative spikes at LES and LAT positions was inconsistent

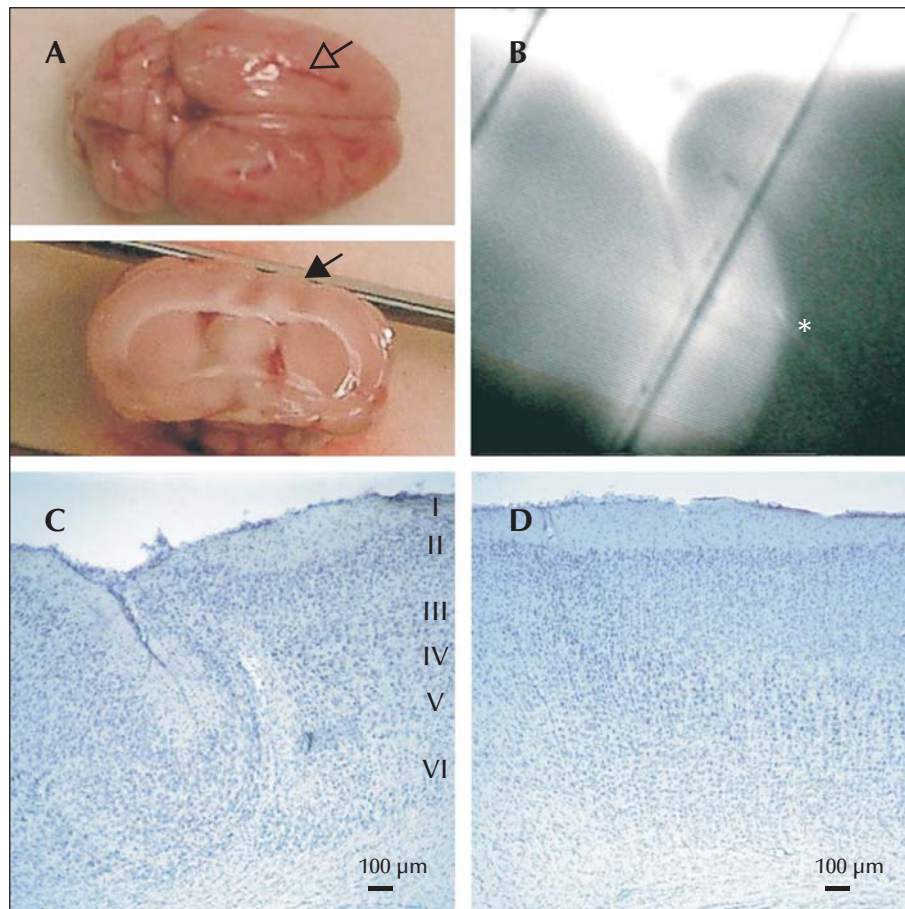


**Figure 1.** Macroscopic and microscopic appearance of the neocortical freeze-induced microsulcus. **A)** The microsulcus is clearly visible macroscopically on the surface of the hemispheric convexity (open arrow) and on coronal cross sections (filled arrow). **B)** Microsulcus in a coronal brain slice from a freeze-lesioned rat, while *in vitro* field potential recordings were performed. The white star shows the position of the recording glass micropipette at the rim of the lesion. **C)** Low-magnification photomicrograph of a cresylecht violet (CV) Nissl substance-stained coronal section from a freeze-lesioned hemisphere. **D)** Low-magnification photomicrograph of a CV-stained coronal section from a sham-operated (control) rat.

(figure 3A; right traces). Discharges recorded from LES and LAT positions did not differ in any of the parameters measured (latency, repetition rate, maximum amplitude, burst integral). The latency time to first appearance of epileptiform activity was  $24 \pm 6$  min for the FL slices ( $n = 5$ ) and  $33 \pm 8$  min for the CTRL slices ( $n = 5$ ). The difference was not significant ( $p = 0.21$ ).

EFP recorded from FL slices occurred at an average repetition rate of  $3.3 \pm 0.6 \text{ min}^{-1}$ , which was not different from the EFP repetition rate in CTRL slices ( $3.3 \pm 0.4 \text{ min}^{-1}$ ; figure 3A, B; left traces). In both FL and CTRL slices, single discharges consisted of an initial negative spike, followed by a repolarization phase (figure 3A, B; right traces). In FL slices, the repolarization phase was prolonged, with superimposed afterdischarges, giving the discharges the appearance of ictal-like events (figure 3A; right traces). In CTRL slices, the repolarization phase was shorter; these discharges were of the interictal type (figure 3B; right

trace). EFP in FL slices had a slightly, although not significantly, higher, maximum burst amplitude than EFP recorded from CTRL slices ( $480 \pm 130 \mu\text{V}$ , compared to  $210 \pm 60 \mu\text{V}$ ,  $p = 0.1$ ). The average burst integral was significantly higher in FL slices than in CTRL slices ( $1220 \pm 324 \mu\text{Vs}$ , compared to  $261 \pm 117 \mu\text{Vs}$ ,  $p = 0.02$ ).

## Discussion

Our current results show dissociation between the expression of *in vitro* hyperexcitability and the occurrence of *in vivo* epileptogenicity in pathologically-confirmed dysplastic neocortical lesions in the rat. In our study, we were able to consistently induce a focal cortical lesion by applying a freeze probe to the skull of newborn rat pups. The histological appearance and structure of these lesions are consistent with the findings originally reported Dvorak

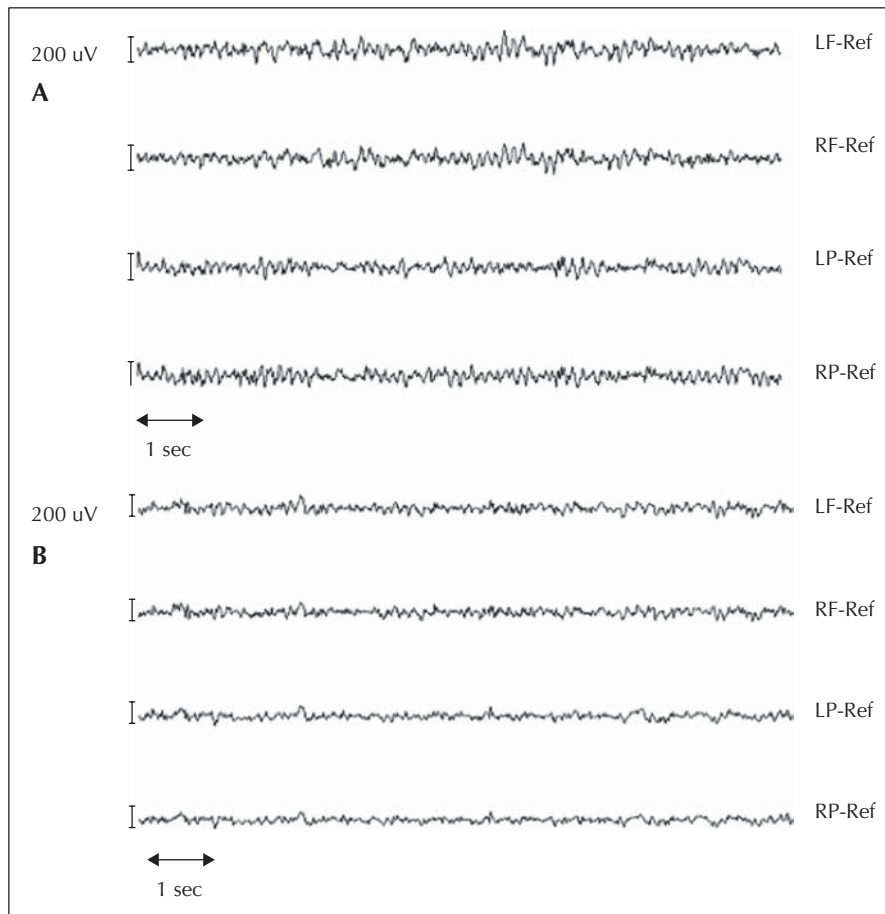


**Figure 2.** Representative normal EEG recordings at resting stage at approximately day 10 after PTZ-injection: **A)** freeze-lesioned rat, **B)** control rat. LF = left frontal, RF = right frontal, LP = left parietal, RP = right parietal, REF = reference electrode (frontal sinus).

and Feit (Dvorak and Feit, 1977, Dvorak *et al.* 1978) that were subsequently replicated by different groups (DeFazio and Hablitz, 2000, Ferrer *et al.* 1993, Holmes *et al.* 1999, Luhmann and Raabe, 1996, Rosen *et al.* 1992).

In spite of the clear lesion, the animals did not develop spontaneous seizures, and long-term EEG recording did not show any epileptiform discharges in the absence of a seizure-provoking agent. Several animal models of focal epilepsy show that not all animals receiving the acute injury actually develop seizures (Bertram and Cornett,

1994, Kellinghaus *et al.* 2004, Kondo *et al.* 2001, Tanaka *et al.* 1985, Möddel *et al.* unpublished observations). Correspondingly, not all human patients with MCD develop epilepsy, even if the malformation is severe (Bertram and Cornett, 1994, Leventer *et al.* 1999), and healthy relatives of epileptic patients with MCD frequently also have subtle cortical abnormalities (Merschhemke *et al.* 2003). We may have monitored an insufficient number of animals for an insufficient amount of time. Nevertheless, the absence of spontaneous seizures (and spontaneous unprovoked interictal spikes) in animals harboring clear

**Table 1.** Induction of seizures by pentylenetetrazole (PTZ) injection in freeze-lesioned, compared to sham-operated control rats.

Variable	Freeze-lesioned rats (n = 10): median (range)	Controls (n = 10): median (range)	Mann-Whitney U-Test
Age at PTZ injection	105 days (90-120 days)	97.5 days (90-105 days)	p = 0.30
Weight at PTZ injection	405 g (305-510 g)	418 g (255-505 g)	p = 0.91
Threshold for seizure stage II/III	37.5 mg/kg (25-70 mg/kg)	40 mg/kg (35-45 mg/kg)	p = 0.26
Threshold for seizure stage IV/V	60 mg/kg (35-80 mg/kg)	45 mg/kg (40-65 mg/kg)	p = 0.07

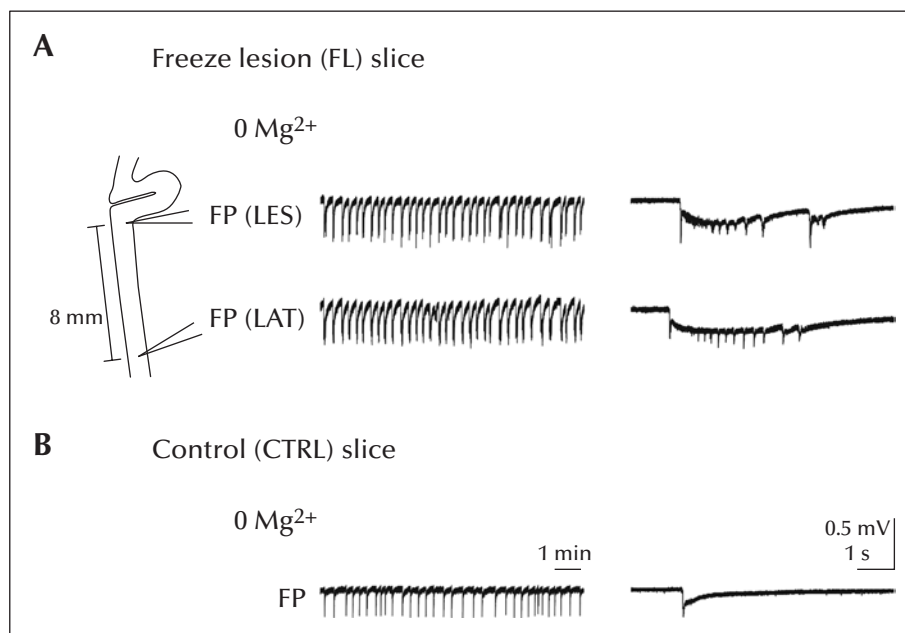


**Figure 3.** Zero-magnesium-induced epileptiform field potentials (EFP) recorded from coronal brain slices from freeze-lesioned rats (FL slices; A), compared to control animals (CTRL slices; B); 10 min periods depicting EFP repetition rate (left traces); single EFP bursts displayed at a higher time resolution (right traces). **A**) Field potentials (FP) recorded from a FL slice. FP were simultaneously recorded from the perilesional cortex in the immediate vicinity of the microsulcus (LES), and from a site 8 mm lateral of the microsulcus (LAT). Zero-magnesium-induced EFP were ictal-like, with an initial negative spike, followed by a prolonged repolarization phase with superimposed afterdischarges. EFP recorded from LES and LAT positions did not differ in terms of repetition rate, maximum amplitude, or burst integral. **B**) FP recorded from a CTRL slice. Zero-magnesium-induced EFP were of the interictal-like type, consisting of an initial negative spike and a slow repolarization phase which was significantly shorter than in FL slices. Calibration bars in B apply to all traces.

neocortical lesions which show *in vitro* hyperexcitability suggests that the development of behavioral seizures may require additional factors other than regional (focal) excitability changes.

Induction of a generalized tonic-clonic seizure by PTZ did not elicit spontaneous epileptiform activity beyond 12 hours after injection. Decreased threshold for PTZ-induced seizures has been demonstrated in different animal models of focal neocortical epilepsy, e.g. the cobalt oxide model in cats (Hoehnerman and Reichenenthal, 1983) and the alumina-gel model in monkeys (Mayanagi and Walker, 1974), and also in a mouse model of cortical dysplasia (Gabel and LoTurco, 2002). However, the threshold for PTZ-induced seizures was not decreased in the freeze-lesioned rats. These results are consistent with those reported by Holmes (Holmes *et al.* 1999), who showed no difference in afterdischarge threshold and kindling rates between freeze-lesioned and control rats using amygdala-kindling. In contrast to the unchanged threshold for PTZ-induced seizures, there is a report of decreased seizure threshold for hyperthermia-induced seizures in immature, freeze-lesioned rats (Scantlebury *et al.* 2004). However, animals lesioned on postnatal day 1 were used, whereas our animals were lesioned within 30 hours after birth, most of them within the first 18 hours

because they were born during the night and the procedure took place the following morning. In a study differentiating between lesions performed on P0 versus P1 found that animals lesioned on P0 showed decreased incidence of epileptiform activity as mature rats, compared to animals treated on P1 (Jacobs *et al.* 1999a), probably due to less extensive retargeting of fibers into the epileptogenic zone if the lesion was induced earlier.

In contrast to the *in vivo* findings that showed no evidence of spontaneous or differentially drug-induced epileptogenicity, our *in vitro* studies confirmed the presence of hyperexcitability in hemispheric brain slices of freeze-lesioned animals, with significantly higher epileptiform field potentials (EFP) burst integrals in FL slices, as compared to CTRL slices. Comparison of EFP recorded from the cortex directly adjacent to the freeze-lesion induced microsulcus (LES), with EFP recorded from the cortex 8 mm lateral to the microsulcus (LAT), showed no differences in any of the parameters measured. Jacobs (Jacobs *et al.* 1999b, Jacobs *et al.* 1999c) found that the epileptogenic region is not located within the lesion proper, but within 0.5-2.5 mm lateral to the lesion, and remains hyperexcitable even if the lesion itself is removed. They suggested that thalamo-cortical and intracortical afferents originally targeting neurons within the lesioned area may

have been redirected to regions adjacent to the lesion, leading to hyperinnervation with excitatory connections (Jacobs and Prince, 2005).

However, our recordings used the zero-magnesium model of epileptiform activity (Avoli et al. 1987, Avoli et al. 1991, Mody et al. 1987). The low-magnesium model induces robust epileptiform activity in both normal and lesioned cortex by augmenting the NMDA-component of the excitatory postsynaptic potential (EPSP), without pharmacological blockade of synaptic receptors (i.e. GABA-A receptors in the bicuculline model). *In vivo* conditions are therefore more closely mimicked, as recurrent and lateral inhibition remains intact. In addition, low-magnesium activity induces postsynaptic calcium influx, resulting in activation of the same calcium-dependent, second messenger mechanisms that underlie activity-dependent neuronal plasticity. Redecker (Redecker et al. 2005) used optical imaging to investigate the epileptiform activity of freeze-lesioned slices produced by the zero-magnesium model. In contrast to the spontaneous activity, epileptiform potentials induced by the omission of magnesium always originated from the more superficial layer of the lesion itself. Zilles (Zilles et al. 1998) reports widespread changes of GABA(A)- and non-NMDA glutamate receptor densities in the lesioned hemisphere including the lesion, whereas changes in GABA(B) and NMDA glutamate receptors were confined to the dysplastic cortex itself. This specific pattern of changes of receptor densities may be responsible for the increased excitability of the lesion itself when magnesium is omitted from the bath solution. Thus, following major changes in general brain excitability as modeled here, different generators of epileptiform discharges may be active. More studies are needed to identify the role of subcortical structures and/or other metabolic (focal or systemic) adaptations of the affected (and potentially epileptogenic) tissue in the development of epileptogenesis. □

**Acknowledgements.** This work was supported in part by the “Innovative Medizinische Forschung” (IMF) of the University of Münster, Germany (IMF scholarships to Christoph Kellinghaus (KE 620201) and Gabriel Möddel (MO 620202), and by the National Institutes of Health (NIH) grant K08 NS02046 and 1R21 NS42354 to Imad M. Najm. Part of the study was published as an abstract at the Annual Meeting of the American Epilepsy Society in Washington, 2005.

## References

- Amano S, Ihara N, Uemura S, et al. Development of a novel rat mutant with spontaneous limbic-like seizures. *Am J Pathol* 1996; 149: 329-36.
- Annegers JF. Epidemiology and genetics of epilepsy. *Neurol Clin* 1994; 12: 15-29.
- Avoli M, Drapeau C, Louvel J, et al. Epileptiform activity induced by low extracellular magnesium in the human cortex maintained in vitro. *Ann Neurol* 1991; 30: 589-96.
- Avoli M, Louvel J, Pumain R, et al. Seizure-like discharges induced by lowering  $[Mg^{2+}]_o$  in the human epileptogenic neocortex maintained in vitro. *Brain Res* 1987; 417: 199-203.
- Baraban SC, Schwartzkroin PA. Electrophysiology of CA1 pyramidal neurons in an animal model of neuronal migration disorders: prenatal methylazoxymethanol treatment. *Epilepsy Res* 1995; 22: 145-56.
- Bast T, Ramantani G, Seitz A, et al. Focal cortical dysplasia: prevalence, clinical presentation and epilepsy in children and adults. *Acta Neurol Scand* 2006; 113: 72-81.
- Bertram EH, Cornett JF. The evolution of a rat model of chronic spontaneous limbic seizures. *Brain Res* 1994; 661: 157-62.
- Chae T, Kwon YT, Bronson R, et al. Mice lacking p35, a neuronal specific activator of Cdk5, display cortical lamination defects, seizures, and adult lethality. *Neuron* 1997; 18: 29-42.
- Chevassus-Au-Louis N, Baraban SC, Gaiarsa JL, et al. Cortical malformations and epilepsy: new insights from animal models. *Epilepsia* 1999; 40: 811-21.
- DeFazio RA, Hablitz JJ. Alterations in NMDA receptors in a rat model of cortical dysplasia. *J Neurophysiol* 2000; 83: 315-21.
- Dvorak K, Feit J. Migration of neuroblasts through partial necrosis of the cerebral cortex in newborn rats-contribution to the problems of morphological development and developmental period of cerebral microgyria. Histological and autoradiographical study. *Acta Neuropathol (Berl)* 1977; 38: 203-12.
- Dvorak K, Feit J, Jurankova Z. Experimentally induced focal microgyria and status verrucosus deformatis in rats--pathogenesis and interrelation. Histological and autoradiographical study. *Acta Neuropathol (Berl)* 1978; 44: 121-9.
- Ferrer I, Alcantara S, Catala I, et al. Experimentally induced laminar necrosis, status verrucosus, focal cortical dysplasia reminiscent of microgyria, and porencephaly in the rat. *Exp Brain Res* 1993; 94: 261-9.
- Gabel LA, LoTurco JJ. Layer I ectopias and increased excitability in murine neocortex. *J Neurophysiol* 2002; 87: 2471-9.
- Hamiwka L, Jayakar P, Resnick T, et al. Surgery for epilepsy due to cortical malformations: ten-year follow-up. *Epilepsia* 2005; 46: 556-60.
- Hocherman S, Reichenthal E. Induction of semichronic epileptic foci using cobalt oxide. *Surg Neurol* 1983; 20: 417-21.
- Holmes GL, Sarkisian M, Ben Ari Y, et al. Consequences of cortical dysplasia during development in rats. *Epilepsia* 1999; 40: 537-44.
- Jacobs KM, Hwang BJ, Prince DA. Focal epileptogenesis in a rat model of polymicrogyria. *J Neurophysiol* 1999; 81: 159-73.
- Jacobs KM, Kharazia VN, Prince DA. Mechanisms underlying epileptogenesis in cortical malformations. *Epilepsy Res* 1999; 36: 165-88.
- Jacobs KM, Mogensen M, Warren E, et al. Experimental microgyri disrupt the barrel field pattern in rat somatosensory cortex. *Cereb Cortex* 1999; 9: 733-44.
- Jacobs KM, Prince DA. Excitatory and inhibitory postsynaptic currents in a rat model of epileptogenic microgyria. *J Neurophysiol* 2005; 93: 687-96.

- Kellinghaus C, Kunieda T, Ying Z, *et al.* Severity of histopathologic abnormalities and *in vivo* epileptogenicity in the *in utero* radiation model of rats is dose dependent. *Epilepsia* 2004; 45: 583-91.
- Kondo S, Najm I, Kunieda T, *et al.* Electroencephalographic characterization of an adult rat model of radiation-induced cortical dysplasia. *Epilepsia* 2001; 42: 1221-7.
- Leventer RJ, Phelan EM, Coleman LT, *et al.* Clinical and imaging features of cortical malformations in childhood. *Neurology* 1999; 53: 715-22.
- Lüders H, Schuele SU. Epilepsy surgery in patients with malformations of cortical development. *Curr Opin Neurol* 2006; 19: 169-74.
- Luhmann HJ, Raabe K. Characterization of neuronal migration disorders in neocortical structures: I. Expression of epileptiform activity in an animal model. *Epilepsy Res* 1996; 26: 67-74.
- Mascott CR, Gotman J, Beaudet A. Automated EEG monitoring in defining a chronic epilepsy model. *Epilepsia* 1994; 35: 895-902.
- Mayanagi Y, Walker AE. Experimental temporal lobe epilepsy. *Brain* 1974; 97: 423-46.
- Merschhemke M, Mitchell TN, Free SL, *et al.* Quantitative MRI detects abnormalities in relatives of patients with epilepsy and malformations of cortical development. *Neuroimage* 2003; 18: 642-9.
- Mody I, Lambert JD, Heinemann U. Low extracellular magnesium induces epileptiform activity and spreading depression in rat hippocampal slices. *J Neurophysiol* 1987; 57: 869-88.
- Paxinos G. The rat brain in stereotactic coordinates. 1986.
- Prayson RA, Estes ML. Cortical dysplasia: a histopathologic study of 52 cases of partial lobectomy in patients with epilepsy. *Hum Pathol* 1995; 26: 493-500.
- Racine RJ. Modification of seizure activity by electrical stimulation. II. Motor seizure. *Electroencephalogr Clin Neurophysiol* 1972; 32: 281-94.
- Redecker C, Hagemann G, Köhling R, *et al.* Optical imaging of epileptiform activity in experimentally induced cortical malformations. *Exp Neurol* 2005; 192: 288-98.
- Roper SN, Gilmore RL, Houser CR. Experimentally induced disorders of neuronal migration produce an increased propensity for electrographic seizures in rats. *Epilepsy Res* 1995; 21: 205-19.
- Rosen GD, Press DM, Sherman GF, *et al.* The development of induced cerebrocortical microgyria in the rat. *J Neuropathol Exp Neurol* 1992; 51: 601-11.
- Scantlebury MH, Ouellet PL, Psarropoulou C, *et al.* Freeze lesion-induced focal cortical dysplasia predisposes to atypical hyperthermic seizures in the immature rat. *Epilepsia* 2004; 45: 592-600.
- Tanaka T, Kaijima M, Yonemasu Y, *et al.* Spontaneous secondarily generalized seizures induced by a single microinjection of kainic acid into unilateral amygdala in cats. *Electroencephalogr Clin Neurophysiol* 1985; 61: 422-9.
- Tassi L, Colombo N, Garbelli R, *et al.* Focal cortical dysplasia: neuropathological subtypes, EEG, neuroimaging and surgical outcome. *Brain* 2002; 125: 1719-32.
- Taylor DC, Falconer MA, Bruton CJ, *et al.* Focal dysplasia of the cerebral cortex in epilepsy. *J Neurol Neurosurg Psychiatry* 1971; 34: 369-87.
- Wyllie E, Comair YG, Kotagal P, *et al.* Seizure outcome after epilepsy surgery in children and adolescents. *Ann Neurol* 1998; 44: 740-8.
- Zilles K, Qu M, Schleicher A, *et al.* Characterization of neuronal migration disorders in neocortical structures: quantitative receptor autoradiography of ionotropic glutamate, GABA(A) and GABA(B) receptors. *Eur J Neurosci* 1998; 10: 3095-106.